AD-A080 648 FORD MOTOR CO DEARBORN MICH F/G 11/2
X-RAY RADIOGRAPHY OF GAS TURBINE CERAMICS.(U)
OCT 79 D J CASSIDY, M F ELBART N00014-78-C-0714
UNCLASSIFIED NL

END
DATE FILMED
3-80
DDC

12

X-RAY RADIOGRAPHY OF GAS TURBINE CERAMICS

Technical Report By:
D. J. Cassidy, M. F. Elgart
Ford Motor Company,
Dearborn, Michigan 48121

Date: October 20, 1979
Annual Report No. 1
October 1, 1978 to September 30, 1979
Contract Number N00014-78-C-0714
Contract Authority Number NR032-590/6-28-78 (471)

Sponsored by the
Office of Naval Research
Department of the Navy
Arlington, Virginia 22217

UNCLASSIFIED

SECURITY CLASSIFICATION OF THIS PAGE (When Data Entered)

REPORT DOCUMENTATION PAGE	READ INSTRUCTIONS BEFORE COMPLETING FORM
1. REPORT NUMBER: 1	2. GOVT ACCESSION NO.
3. RECIPIENT'S CATALOG NUMBER	
4. TITLE (and Subtitle): X-Ray Radiography of Gas Turbine Ceramics	5. TYPE OF REPORT & PERIOD COVERED: Annual Report, NR-1, 1 Oct. 1978 — Sept. 1979
6. PERFORMING ORG. REPORT NUMBER	
7. AUTHOR(s): D. J. Cassidy, Engineering and Research Staff — Research; M. F. Elgart, Engineering and Research Staff — Research	8. CONTRACT OR GRANT NUMBER(s): N 000-14-78-C-0714
9. PERFORMING ORGANIZATION NAME AND ADDRESS: Ford Motor Company, Dearborn, Michigan, 48121	10. PROGRAM ELEMENT, PROJECT, TASK AREA & WORK UNIT NUMBERS
11. CONTROLLING OFFICE NAME AND ADDRESS: Office of Naval Research, 800 North Quincy Street, Arlington, Virginia 22217	12. REPORT DATE: 20 Oct. 1979
	13. NUMBER OF PAGES: 22
14. MONITORING AGENCY NAME & ADDRESS (if different from Controlling Office)	15. SECURITY CLASS. (of this report): Unclassified
	15a. DECLASSIFICATION/DOWNGRADING SCHEDULE

16. DISTRIBUTION STATEMENT (of this Report)

Approved for public release; distribution unlimited.

17. DISTRIBUTION STATEMENT (of the abstract entered in Block 20, if different from Report)

18. SUPPLEMENTARY NOTES

19. KEY WORDS (Continue on reverse side if necessary and identify by block number)

Ceramics
Silicon Nitride
Non Destructive Evaluation
X-Ray Radiography
Tomography
Image Enhancement
Image Reconstruction

20. ABSTRACT (Continue on reverse side if necessary and identify by block number)

See following page.

DD FORM 1 JAN 73 1473 EDITION OF 1 NOV 65 IS OBSOLETE

UNCLASSIFIED

SECURITY CLASSIFICATION OF THIS PAGE (When Data Entered)

141250

ABSTRACT

This program was conceived for the purpose of investigating X-ray radiography and X-ray tomography in the detection of gross fabrication flaws in complex-shaped ceramic components such as those currently under development for advanced high temperature turbine engines.

The first year effort of the program was directed towards (1) the fabrication of ceramic test coupons with defects of known size and shape, (2) the establishment of baseline data for the resolution of these defects using Microfocus X-ray equipment, (3) the definition of equipment concepts for a computer assisted tomography (CAT) system; and (4) the development of a CAT algorithm.

Silicon nitride coupons with slot type defects (25-175 microns) and circular shaped defects (25-1000 microns) were fabricated. Baseline data were obtained from these test coupons using Microfocus X-ray and image enhancement techniques.

A Computer Assisted Tomography (CAT) design concept was defined, which employs a computer-operated rotary stage, intensifying screen or X-ray film, TV camera, computer, digital image analyzer, and TV monitor.

Computer reconstruction algorithms were investigated with respect to CAT and a preferred approach was determined. An appropriate CAT algorithm was written and tested.

FOREWORD

This report describes work completed on X-ray radiography and tomography during the first year of a program sponsored by the Office of Naval Research, Contract N00014-78-C-0714.

This contract with the Ford Motor Company, Dearborn, Michigan, is being performed under the technical monitoring of Dr. Robert Pohanka, Scientific Officer, Department of the Navy, Washington, D.C.

Ford personnel contributing to this phase of the program are: D. J. Cassidy, Program Manager; M. F. Elgart, Principal Investigator; A. F. McLean, Mgr., Ceramic Materials Department; R. Terhune, D. D. Dodge; E. A. Fisher, S. A. Zyck, C. Bodurow, C. M. W. Lehman, A. T. Vulpetti, L. Bartosiewicz; J. L. Bomback. In addition, the authors would like to acknowledge the assistance rendered by the Staff of the Department of Radiology, Henry Ford Hospital, Detroit, Michigan.

TABLE OF CONTENTS

Page

- Report Documentation Page i
- Abstract ii
- Foreword iii
- Table of Contents iv
- List of Figures v

1.0 Purpose of Work 1

2.0 Introduction 1

3.0 Work Plan 1

4.0 Program Status 2

4.1 CAT Equipment Concept 2

4.2 Ceramic Test Coupon Preparation 5

4.3 Development of CAT Algorithms 6

4.4 Radiography and Image Enhancement of Ceramic Test Specimens 9

5.0 Future Work 15

6.0 References 16

LIST OF FIGURES

Figure 1. X-Ray Radiograph of Silicon Nitride Gas Turbine Rotor Ring.

Figure 2. Computer Assisted Tomogram of Silicon Nitride Gas Turbine Rotor Ring.

Figure 3. CAT Equipment Concept

Figure 4. Silicon Nitride Coupon With Slot Type Defect.

Figure 5. Silicon Nitride Coupons and Turbine Rotor Blade with Known Defects.

Figure 6. CAT Coordinate System

Figure 7. Reconstructed Image of Test Object "D"

Figure 8. Reconstructed Image of Test Object "D" with External Defect.

Figure 9. Reconstructed Image of Test Object "O" with Internal Defect.

Figure 10. Image Enhancement of Standard Microfocus Radiograph.

Figure 11. Magnification Radiograph with Image Enhancement.

Figure 12. Slot Coupon "C" Radiograph before Grinding.

Figure 13. Slot Coupon "C" Radiograph after Grinding.

Figure 14. Surface Crack of Rotor Blade 14.

1.0 PURPOSE OF WORK

The purpose of this work is to investigate X-ray radiography and X-ray tomography for the detection of gross fabrication flaws (25-50 microns) in complex-shaped ceramic materials.

2.0 INTRODUCTION

Ceramic materials such as silicon nitride and silicon carbide are emerging as potential future engineering materials. The incentives to develop such materials are the exploitation of vastly abundant raw materials and the exploitation of materials with unique properties such as high refractoriness, high strength at temperature and corrosion/erosion resistance. In particular, development of ceramic materials, fabrication processes, ceramic design methodology and testing methods is receiving widespread attention for application to large utility turbine engines, military turbines and automotive turbine, Diesel and Stirling engines. While considerable progress is being made and actual ceramic components have been succesfully tested in turbine engines[1-13], a key to success in the practical, commercial utilization of ceramics is the ability to non-destructively evaluate ceramic components.

A number of NDE techniques[14,15] are being considered or have been investigated under government sponsorship to detect minute Griffith-type inclusions or flaws in simple shaped ceramic specimens. These include conventional ultrasonics (45 MH_Z), very high frequency ultrasonics (250 MH_Z), neutron radiography, Microfocus X-ray, image enhancement, microwave, thermography and, for surfaces, dye penetrants and photo-acoustic Microscopy. Production-type application of these techniques to rigorously inspect complex shaped ceramic components only appears likely where the component is machined from a solid ceramic block which is quality checked by the particular NDE technique prior to machining. However, the impetus of ceramic processing development is to manufacture complex-shaped parts directly to near net shape. Examples of near net shape processes are injection molding and slip casting of gas turbine rotor blade rings[6,7].

A viable NDE technique for directly-formed ceramic components should meet two major criteria: (1) it should be able to detect fabrication flaws (gross defects as compared to Griffith-type flaws) to ensure that selected components have a material quality equal to test specimen quality used for the determination of design data, and (2) it should be able to examine a complex shaped part in a practical manner. X-ray radiography, combined with digital image (computer) processing (tomography), has the potential to meet these criteria. While state-of-the-art X-ray radiography, is being used to screen ceramic components, it is time-consuming and not practical for complex shapes. This program to develop and optimize X-ray radiography and digital processing techniques is recommended to meet the requirements of a practical NDE method for complex components.

Impetus for the development of computer-assisted tomography (CAT) as a tool for non-destructive evaluation of ceramic turbine components came from an examination of a ceramic rotor ring on an E.M.I. Ltd. brain scanner at Henry Ford Hospital[16]. A normal X-ray radiograph was made of this rotor ring and is shown in Figure 1. A rather large internal void at the rim can be readily seen. If this void extended into the rim, a failure of the rotor could be anticipated. This information could not be obtained from the radiograph. The ceramic part was then analyzed by CAT. These results are shown in Figure 2. The top tomogram is very similar to a normal radiograph. The middle tomogram is a diameter "slice" of the rotor through the large defect. The bottom tomogram shows the outside edge of the rotor at the defect. Together, these tomograms show that the defect extends into the rim of this ceramic rotor.

This study indicates the potential of CAT for non-destructive examination of ceramic parts. While it is obvious that much more information is available using the technique of CAT, the equipment used was not optimized for ceramic materials and was also considered to be excessively costly. Nevertheless, the results were encouraging and prompted the need for a relatively low cost tomographic apparatus specifically designed for ceramics which could provide the necessary non-destructive quality assurance for ceramic parts.

3.0 WORK PLAN

The primary objective of this research is the assessment of computer-assisted tomography as a practical non-destructive evaluation technique for complex-shaped ceramic components. The technique of CAT will be di-

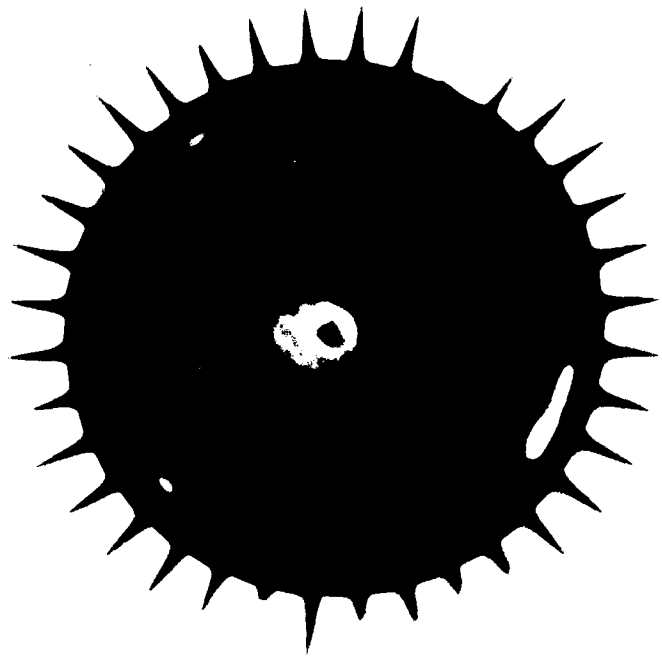

Figure 1. X-Ray Radiograph of Silicon Nitride Gas Turbine Rotor Ring.

rectly compared to standard radiography and image enhanced radiographs in an attempt to quantify defect resolution in ceramic parts. To accomplish this objective, the following steps were planned:

1. Determination of equipment needs to accomplish objectives.
2. Preparation of ceramic test specimens for quantitative evaluation of defect resolution.
3. Development of CAT algorithms for ceramic NDE.
4. Evaluation of ceramic test specimens using microfocus radiography with and without image enhancement.

These steps have been completed or are in progress and will be reported upon in the appropriate sections of this report.

4.0 PROGRAM STATUS

4.1 CAT EQUIPMENT CONCEPT

Careful consideration of equipment requirements, with reference to existing medical machines, has resulted in a novel, relatively-low cost design for CAT of ceramic objects. The equipment concept is shown in Figure 3.

A Microfocus X-ray tube and generator system, manufactured by Magnaflux Corporation is used as the source of penetrating radiation. Since the reduction of focal-spot size increases image resolution and reduces the parallax effects affecting geometric sharpness, the use of a variable focal-spot X-ray system for NDE of ceramic components is required to obtain resolution of very small defects.

In medical applications of CAT, the patient remains in a fixed position while the source and detector system rotate on a special gantry. This is a very costly part of the system, but is not necessary for examination of inanimate objects. By fixing the source-detector geometry, the ceramic component can be rotated and translated through the X-ray field to produce the necessary data for tomographic image reconstruction. An Aerotech movable table with rotary stage was chosen to provide specimen movement.

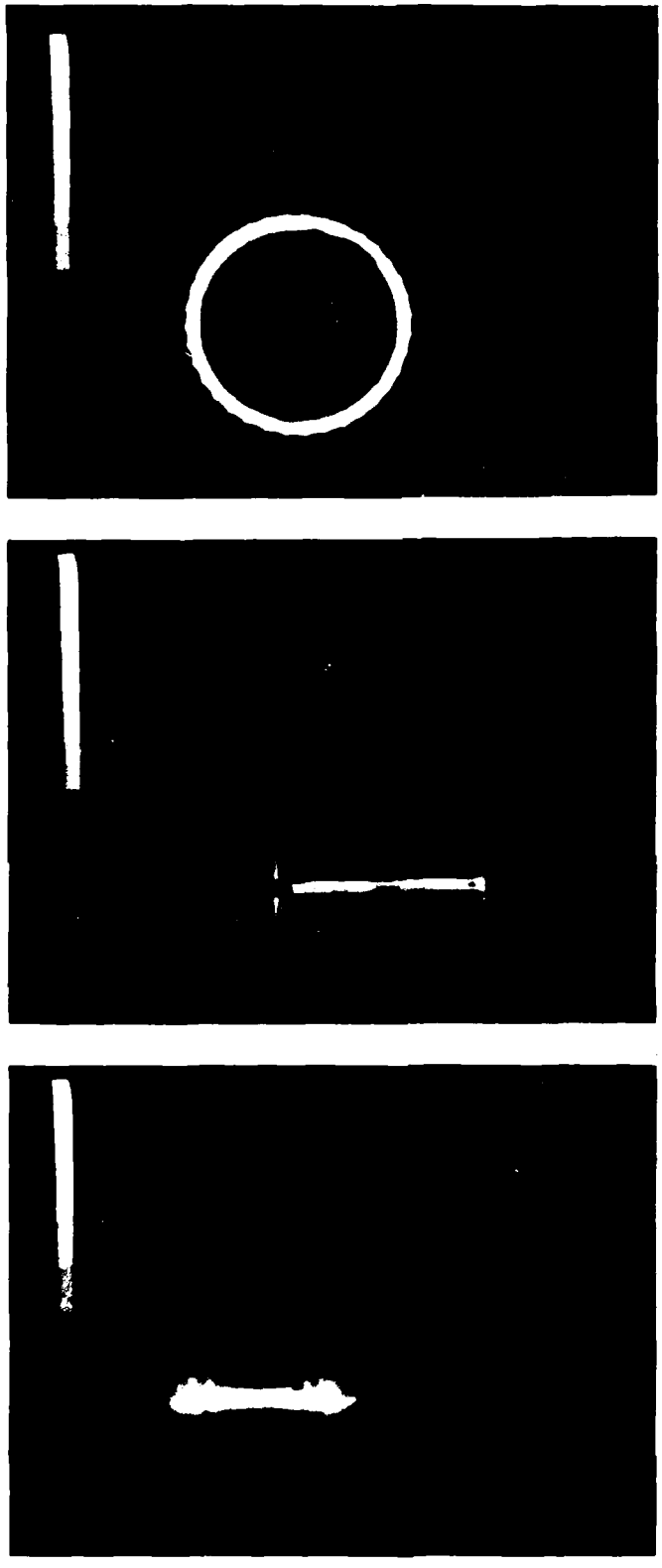

Figure 2. Computer Assisted Tomogram of Silicon Nitride Gas Turbine Rotor Ring.

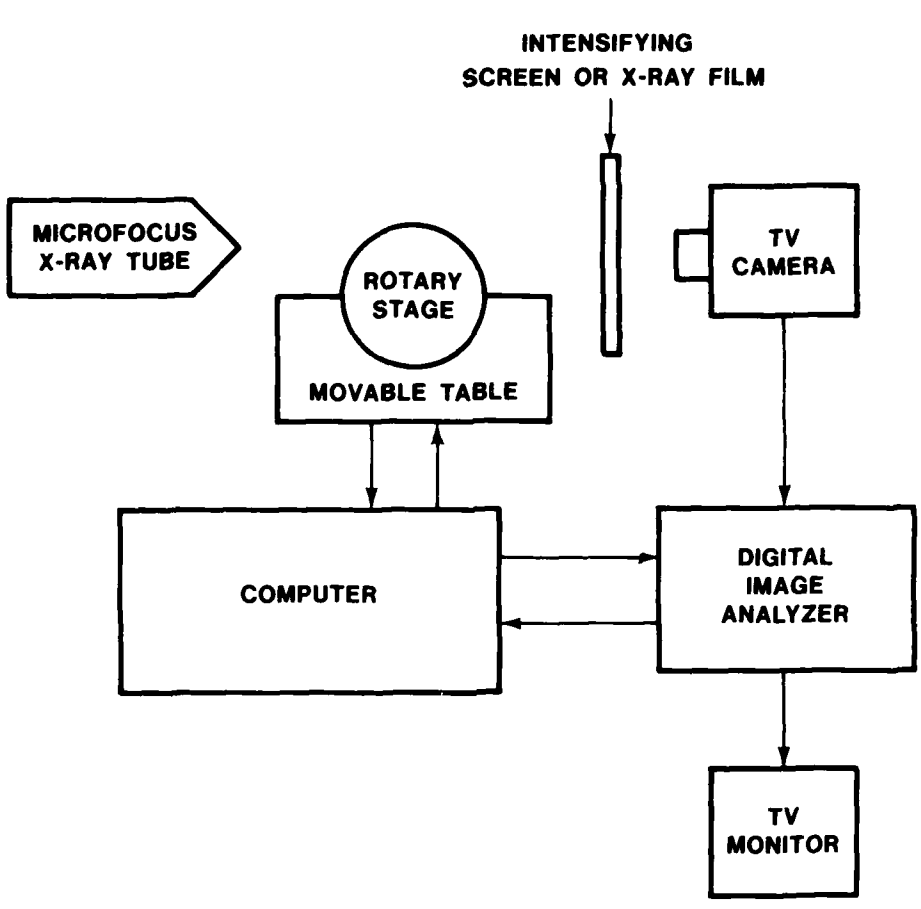

Figure 3. CAT Equipment Concept

The detector used to amass the necessary data for reconstruction has varied from single scintillation detectors to linear arrays of proportional detectors to film. The use of film is most interesting because full three-dimensional information becomes available for reconstruction. However, film suffers from the problem of development time, thus preventing real-time NDE of components. The development of frame-memory and high-speed analog-to-digital converters has now suggested a "filmless" detector which provides a digital image of the component in real-time. The basis for the proposed detector system is a digital image analyzer (Quantex Corp.). This digital image analyzer converts a TV video frame into a 512 x 512 digital image in 0.03 seconds. The 512 x 512 pixels can be accessed by a special purpose computer to provide the necessary data for multiple 2-dimensional image reconstruction. The digital image analyzer thus permits the use of an X-ray intensification screen and television camera combination as a novel detector for CAT.

An additional advantage of the digital image analyzer is that the frame memory can be continuously swept to produce an image for a TV monitor. This provides a simple way of visually inspecting a reconstructed image matrix.

In summary, the following steps are proposed for NDE of ceramic components:

1) Radiographic images at various angles are digitized and stored in a computer.

2) The various tomographic cross-sections are reconstructed and stored.

3) The reconstruction matrix is transferred to the digital image analyzer for visual inspection on a TV monitor.

Initially, CAT work will involve the use of X-ray film as the detector and data storage medium. The use of film in this way will permit the comparison of microfocus radiography and CAT development to proceed on schedule. Ultimately, intensifying screens will be used for a CAT real time inspection system.

4.2 CERAMIC TEST COUPON PREPARATION

One group of reaction bonded silicon nitride coupons with known defects was fabricated by slip casting a 100 x 50 x 6.5 mm shape with slot type defects of 25, 75, 125, and 175 microns width and approximately 3 mm depth. This casting was then processed via state of the art nitriding technique[11].

After nitriding to a density of 2.7 g/cc, the specimen was sectioned into coupons 6.5 x 6.5 x 25 mm resulting in 4 individual coupons with varying slot widths but the same slot depth of 3 mm and slot length of 3 mm. Figure 4 shows a typical coupon made in this manner. Subsequently, the slot depths of these coupons were systematically reduced to 250 microns for the purpose of determining the ultimate capability of the microfocus X-ray equipment and image enhancement techniques. These data could then be used to compare directly with CAT data.

Silicon nitride blanks were also used to make test bars containing holes drilled to specific diameters and depths. Two types of test coupons were fabricated in this manner. The first type contained holes with diameters equal to their depths, namely, 125, 250, 500, and 1000 microns.

The second type had holes 25, 50, 75, 100, and 125 microns in diameter and approximately 75 microns in depth. In addition, the blades of a silicon nitride turbine rotor were removed to provide test objects containing linear surface cracks. These additional test specimens are displayed in Figure 5.

Figure 4. Silicon Nitride Coupon With Slot Type Defect.

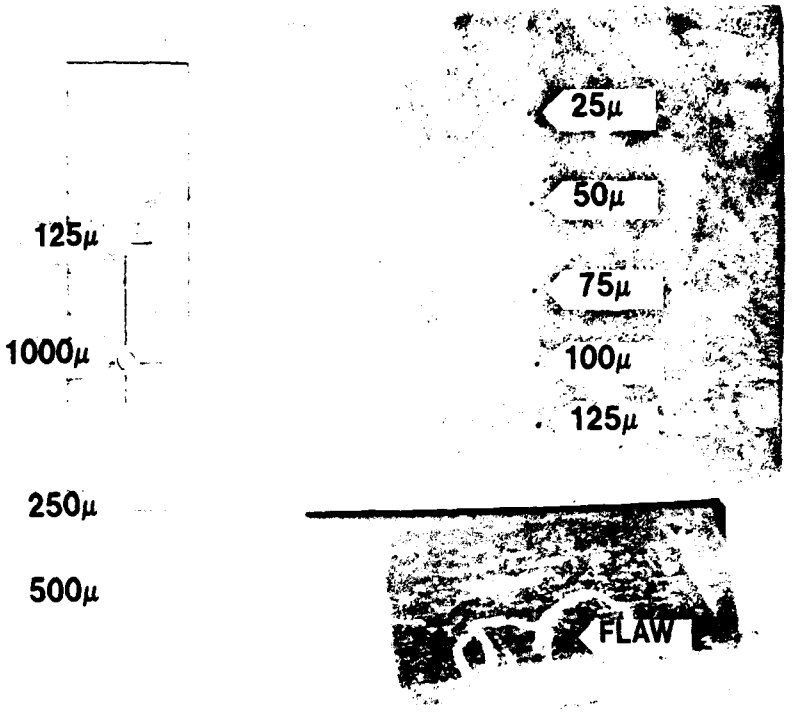

Figure 5. Silicon Nitride Coupons and Turbine Rotor Blade with Known Defects.

4.3 DEVELOPMENT OF CAT ALGORITHMS

Computer-assisted tomography (CAT), often referred to as computerized tomography (CT) or more specifically, as computerized transverse axial tomography (CTAT), is now widely recognized as an important diagnostic technique in medicine. Modern medical diagnostic equipment (commonly known as "brain-scanners" or "whole-body scanners") based on the CAT technique have been used extensively for standard hospital procedures. This remarkable advance in diagnostic medicine is generally attributed to G.N. Hounsfield[17] of EMI Ltd., Great Britain, who designed and built the first practical brain-scanner in 1971.

The technique of digital image reconstruction was first used in radio-astronomy by Bracewell[18] to map the emission of microwave radiation at the surface of the sun. The technique was also developed for transmission electron microscopy by DeRosier and Klug [19] and Gordon, et al[20]. However, emphasis for development of this technique to date still resides primarily within medical applications.

Three main classes of algorithms have evolved to provide solutions for the CAT technique. These include Fourier-convolution methods, [21, 22, 23] spatial back-projection with filtering, [24, 25] and iterative reconstruction methods. [26, 27, 28] Two important differences between medical applications and CAT of ceramics are readily discernible. The linear attenuation coefficients of defects and ceramic materials are quite different; in medical applications, the linear attenuation coefficients of parts of the head may differ by only 0.5%. Secondly, with respect to ceramic objects, the shape of the object and the linear attenuation coefficient of the specific ceramic material can be quite accurately determined, thus providing significant information for use in an algorithm. For these reasons, an iterative, spatial back-projection algorithm was determined to be most appropriate for the NDE of ceramics.

The coordinate system proposed for the CAT technique is shown in Figure 6. The source and detector are fixed, defining the image space. The object can be rotated and translated through this image space to provide the initial raw data. For X-ray transmission measurements, the measurement of the X-ray intensity is related to the sum of the linear attenuation coefficients, $\mu_{x,y}$, of the pixels in image space. The image space can be broken up into a series of rays, which are geometrically determined by the minimum spatial resolution of the detector and the

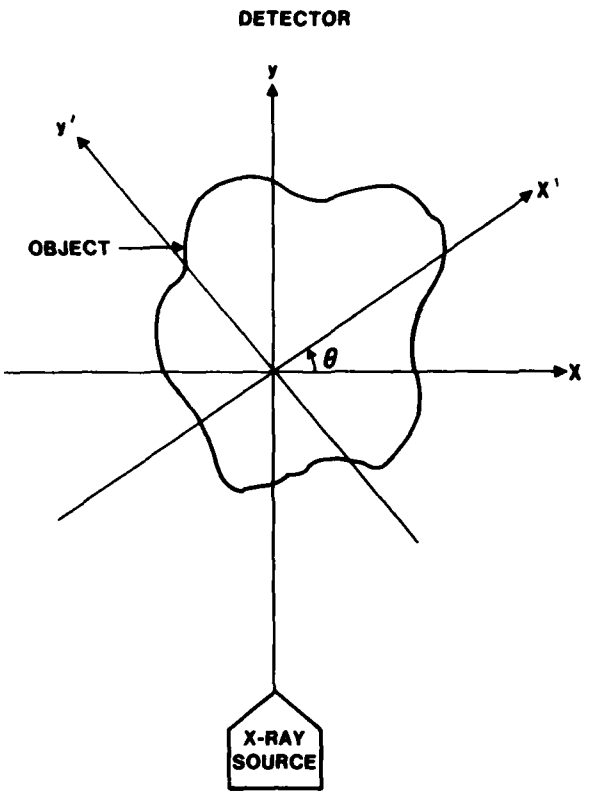

Figure 6. CAT Coordinate System

relative positions of source and detector. The data are collected in the object plane (x',y' coordinates) and then geometrically corrected to the equivalent pixels in the image plane (x,y coordinates) where reconstruction takes place. For a specific ray, the measured intensity of the transmitted X-ray beam is given by

$$I = I_0 \exp\left[-\sum_{i,j} w_{x,y}\,\mu_{x,y}\right] \tag{1}$$

where: I_0 = incident beam intensity
I = transmitted beam intensity
i,j = coordinates of the pixel (x,y) in the transmitted beam.
$w_{x,y}$ = fraction of pixel (x,y) in the transmitted beam.
$\mu_{x,y}$ = linear attenuation coefficient of pixel (x,y).

Equation (1) can be rearranged to give

$$\ln\frac{I_0}{I} - \sum_{i,j} w_{x,y}\,\mu_{x,y} = 0 \tag{2}$$

With the restrictions

$$0 \le w_{x,y} \le 1 \tag{3a}$$

and

$$0 \le \mu_{x,y} \le \mu\text{maximum}, \tag{3b}$$

equation (2) can be evaluated from $\theta = 0°$ to $\theta = 180°$ to provide an image reconstruction from the various ray-sums.

Iterations of this spatial back-projection algorithm are performed until equation (2) is satisfied. For actual data, equation (2) would be modified to give

$$\ln\frac{I_o}{I} - \sum_{i,j} w_{x,y}\,\mu_{x,y} < \sigma \qquad (4)$$

where: σ = standard deviation of the measured beams, I_o and I

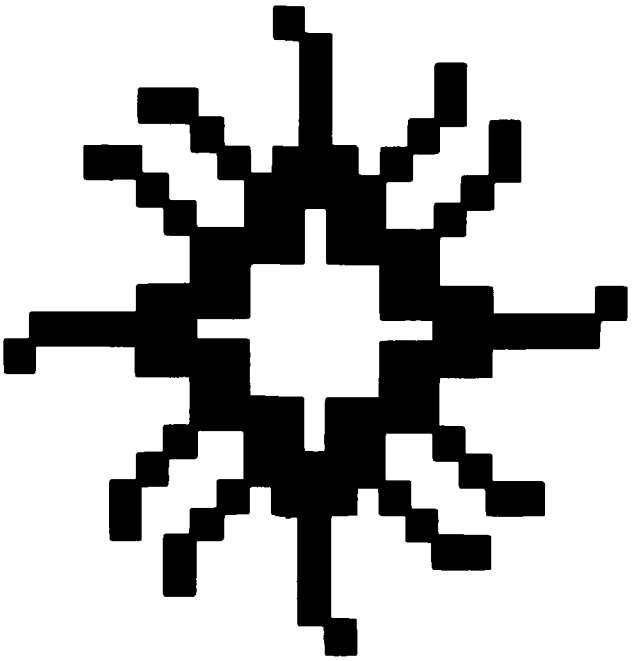

Figure 7. Reconstructed Image of Test Object "D"

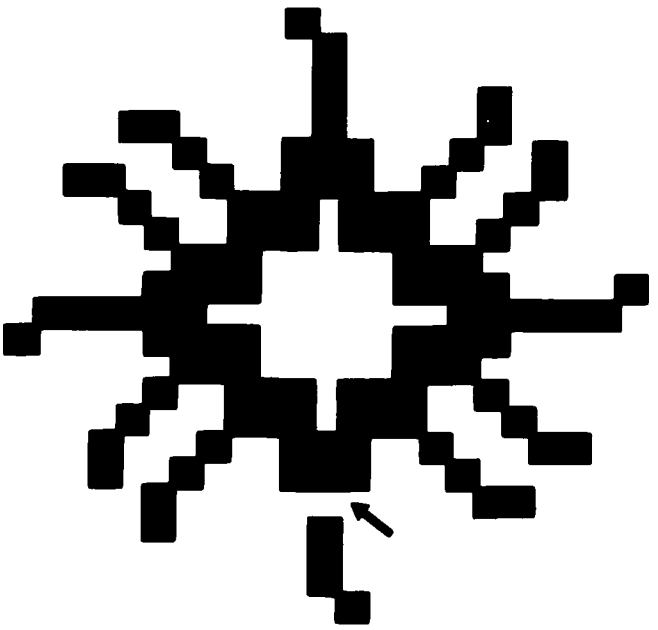

Figure 8. Reconstructed Image of Test Object "D" with External Defect.

This algorithm was tested on the DEC-10 computer system at the Scientific Research Laboratories. Using first principles and equation (1), a series of transmitted beam values were generated for various shapes. These data were then used to reconstruct an image of the original object, utilizing the stated strategy. Figure 7 is the reconstructed image of one of the test objects. Figures 8 and 9 show the reconstructed image of this test object with an external defect and an internal defect, respectively.

Work is continuing on the improvement of this algorithm with regard to accuracy and speed. Conversion to a polar coordinate system is underway because of a possible decrease in computer processing time. Various mathematical filters are under development to help increase the accuracy of the deconvolution procedure. The present algorithm will serve as a baseline for the development of other improved algorithms.

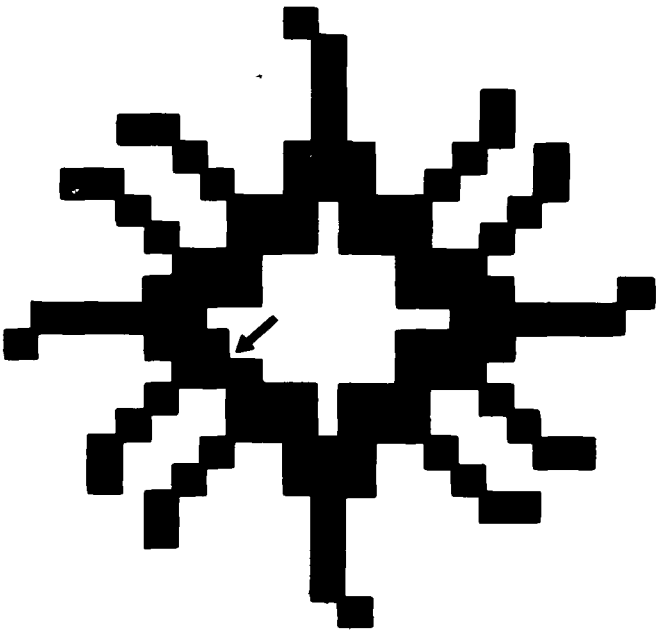

Figure 9. Reconstructed Image of Test Object "O" with Internal Defect.

4.4 RADIOGRAPHY AND IMAGE ENHANCEMENT OF CERAMIC TEST SPECIMENS

X-ray radiography is a widely accepted technique for nondestructive evaluation of defects in materials. The potential for increased use of ceramic components, with much smaller strength-controlling defects, has necessitated a reevaluation of the radiography technique with respect to identification of smaller defects (on the order of 25 microns or less) found, for example, in silicon nitride. Standard radiography and magnification radiography of several types of test coupons were investigated with image enhancement of the radiographs to provide a basis of comparison with the proposed future work using CAT techniques.

Operating parameters were optimized to produce radiographs of density 2.0 - 3.0 by applying the following basic criteria:

a) Beam Voltage

The most important factor in achieving good image quality is the beam voltage. The linear attenuation coefficients of the elements in a material for monochromatic radiation are related to the change in beam intensity by equation (5):

$$I = I_0 \exp(-\mu x) \qquad (5)$$

where: I_0 = incident beam intensity
I = emitted (attenuated) beam intensity
μ = linear attenuation coefficient
x = thickness of the material

Since standard systems for radiography produce a continuous spectrum of X-ray energies, the linear attenuation coefficient is more easily determined by direct experiment. Since the difference for μ(ceramic) and μ(void) is greater at lower X-ray energies, the lowest practical X-ray energies are used for radiography. This corresponds to a voltage setting of 40 kV for the tube voltage of the microfocus system.

b) Focal Spot

The finite size of the focal spot affects image resolution. In general, the smaller the focal spot, the less image blurring due to the penumbral effect that is expected. The focal spot diameter was therefore minimized. This resulted in a practical setting of 75-85 microns diameter for the focal spot of the microfocus X-ray tube.

c) X-ray Flux

The operating characteristics of the specific X-ray tube used will limit the anode current, which is directly proportional to the X-ray flux. Increased beam intensity, and hence shorter irradiation times, occur at higher mA settings. A practical maximum of 0.2 mA current resulted in exposure times of 3-5 minutes.

Magnification radiography occurs when the object is placed at some point between the X-ray tube and film. The amount of magnification is given by equation (6):

$$\text{Magnification} = \frac{\text{film-to-tube distance}}{\text{object-to-tube distance}} \qquad (6)$$

To produce magnified radiographs, a sample table was attached to a lathe table, thus allowing accurate control of the object position. Magnification radiographs in the range of 4X - 8X could then be obtained.

Since computer facilities appropriate to tomography were not yet available, some image enhancement of radiographs was accomplished utilizing the capabilities of the Quantex digital image analyzer. The most successful results were obtained by the following steps:

1) The radiograph was placed on a high-intensity light box.

2) Consecutive TV frames were added together until the limit of the Quantex's frame memory was reached (approximately 18 frames for the 12 bit memory and 8 bit ADC).

3) The TV camera was defocused and approximately 75% of the number of frames collected in step b) were subtracted from the total.

4) The resulting image was displayed, with appropriate modification of the output transform to display all gray levels.

This procedure subtracts a background from the radiograph of interest, producing relative enhancement of film density differences.

Standard radiography of the test coupon containing the 125-1000 microns hole-type defects indicated a practical lower limit for defect resolution of 500 microns. The 250 microns defect could be readily seen by image enhancement of the same radiograph. An illustration of this effect can be seen in Figure 10, which shows an approximate 2X increase in sensitivity with image enhancement. This increase in sensitivity has been found to be approximately constant (2X) for the specific image enhancement technique utilizing the digital image analyzer and lens defocussing.

Magnification radiography provides additional sensitivity for defect resolution when compared to standard radiography. Figure 11 shows an 8X magnification and its enhanced image of the penetrameter used for the previous standard radiography. The 250, 500, and 1000 microns defects are clearly visible on this radiograph. The 125 microns defect is faintly visible in the enhanced radiograph.

It is anticipated that the slot coupons will play an important role in the evaluation of CAT and radiography. Figure 12 shows slot coupon "C" (nominal slot width 125 microns) at the beginning of the grinding procedure (slot

depth 3 mm). The slot is clearly visible in this radiograph. Figure 13 shows slot coupon "C" at the end of the grinding procedure (slot depth 250 microns). The slot is now barely visible in the radiograph. This kind of defect can accurately help to measure the relative sensitivities of radiography and CAT.

Visual inspection with a low-power stereo magnifier of the rotor blades showed some surface cracking. A closeup of one of these surface cracks is shown in Figure 14. This crack is approximately 6-11 microns wide and 1.75 mm in length. The magnified radiograph of this blade and its image enhancement could not discern this crack, although microdensitometor readings over the area where the crack should be indicated some small change in film density. It is to be anticipated that CAT will be a more effective way of detecting these linear cracks in that, at some angle of view, when the crack is parallel to the beam, an increased beam intensity could provide an adequate means for detection.

Summarizing these results, it can be seen that the limits of resolution of hole-type defects is less than 125 microns. This result was obtained using Microfocus radiography with image enhancement and magnification. In addition, slot-type defects 125 microns in width and 250 microns depth were also resolved using the same techniques. Coupons with slot-type defects less than 125 microns in width will soon be studied.

In future work, this information will be used as base line data for establishing the merits of CAT in the detection of defects in ceramics.

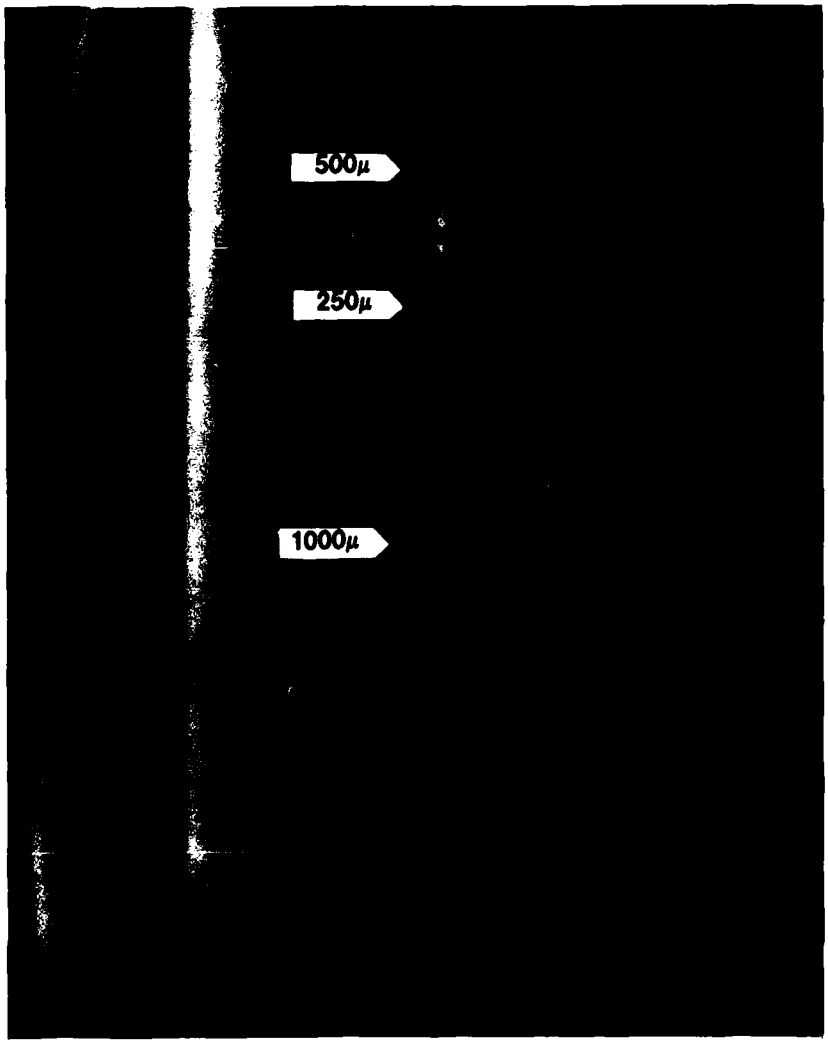

Figure 10. Image Enhancement of Standard Microfocus Radiograph.

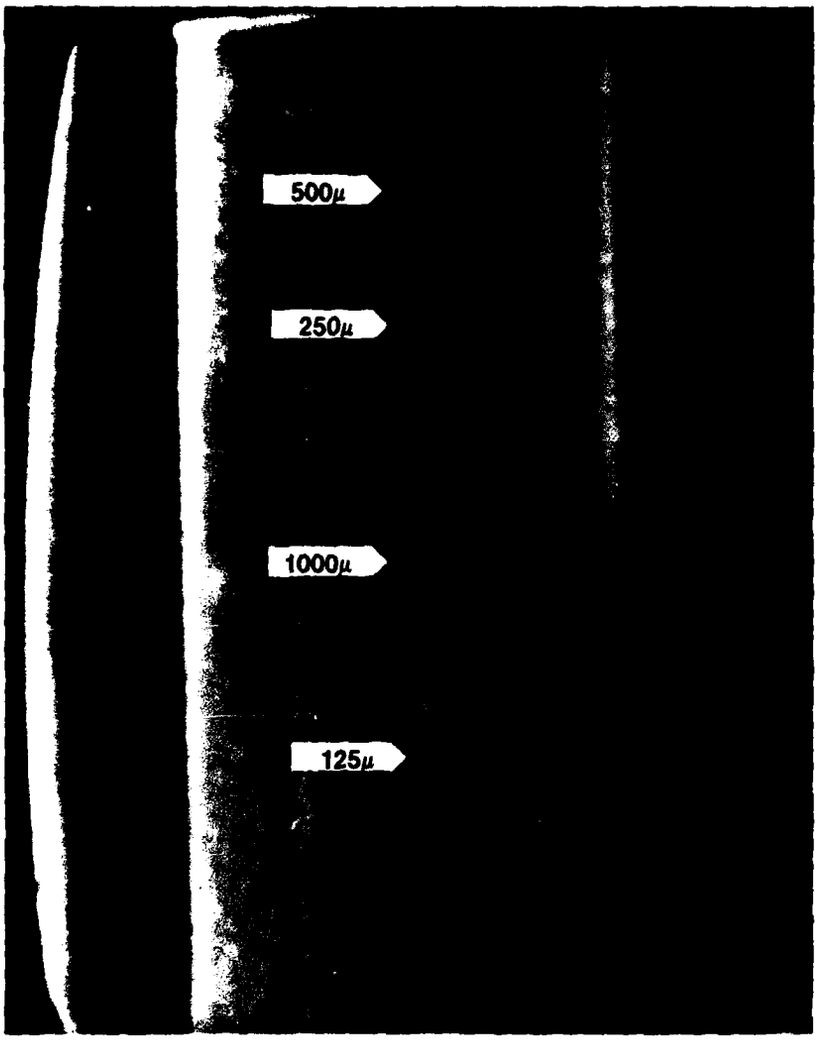

Figure 11. Magnification Radiograph with Image Enhancement.

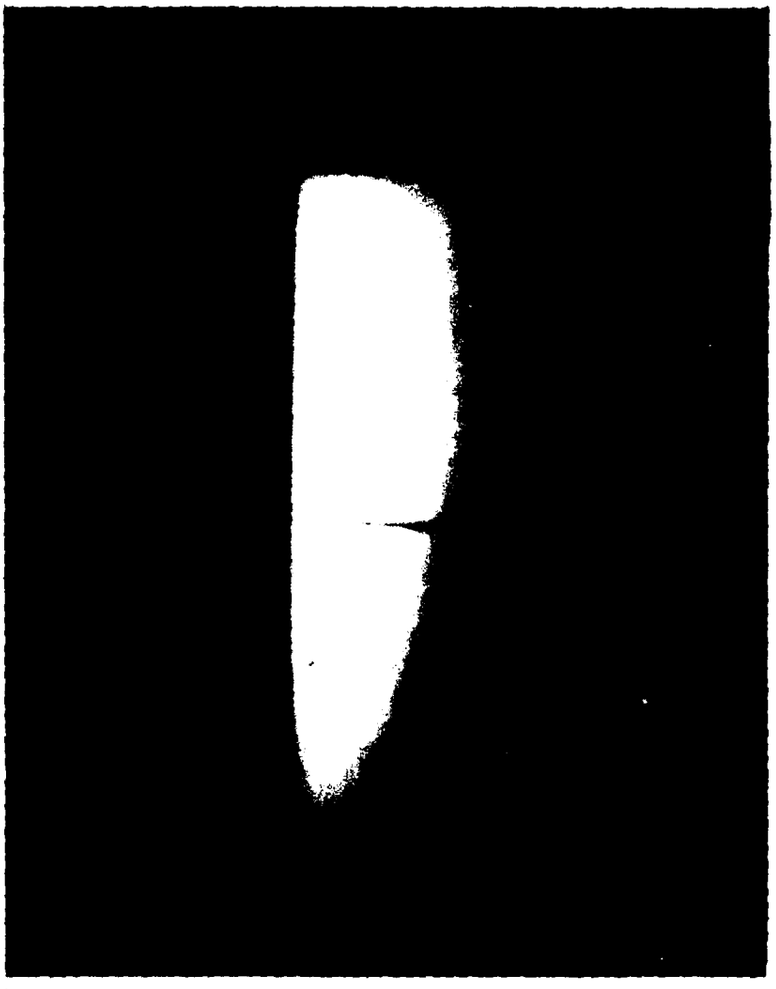

Figure 12. Slot Coupon "C" Radiograph before Grinding.

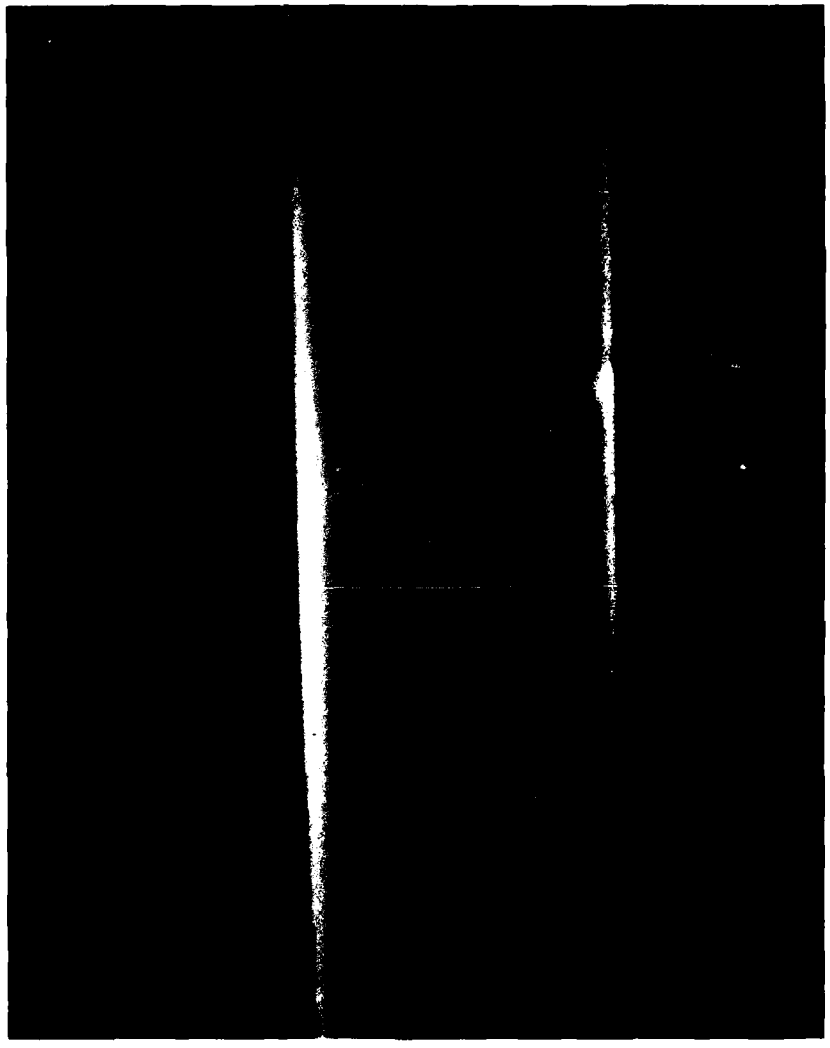

Figure 13. Slot Coupon "C" Radiograph after Grinding.

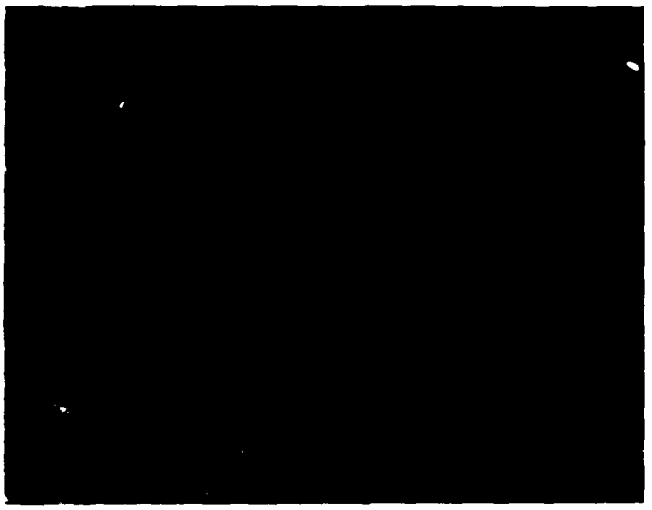

37X

270X

Figure 14. Surface Crack of Rotor Blade 14.

5.0 FUTURE WORK

It is projected that at the conclusion of FY79 the acquisition of base line data using the Microfocus X-ray equipment will be completed. CTAT equipment is expected to be available during FY80. Specifically, the following steps comprise immediate research plans:

1. Assemble and debug apparatus for CTAT.
2. Investigate defects in silicon nitride coupons using CTAT.
3. Optimize parameters for defect resolution using CTAT with silicon nitride coupons.
4. Compare defect resolution of Microfocus X-ray techniques with CTAT methods.
5. Initiate evaluation of X-ray and CTAT techniques with respect to NDE of complex shapes.

6.0 REFERENCES

1. McLean, A. F., Fisher, E. A., Harrison, D. E., "Brittle Materials Design, High Temperature Gas Turbine," AMMRC-CTR-72-3, Interim Report, March, 1972.

2. McLean, A. F., Fisher, E. A., Bratton, R. J., "Brittle Materials Design, High Temperature Gas Turbine," AMMRC-CTR-72-19, Interim Report, September, 1972.

3. McLean, A. F., Fisher, E. A., Bratton, R. J., "Brittle Materials Design, High Temperature Gas Turbine," AMMRC-CTR-73-9, Interim Report, March, 1973.

4. McLean, A. F., Fisher, E. A., Bratton, R. J., "Brittle Materials Design High Temperature Gas Turbine," AMMRC-CTR-73-32, Interim Report, September, 1973.

5. McLean, A. F., Fisher, E. A., Bratton, R. J., "Brittle Materials Design, High Temperature Gas Turbine," AMMRC-CTR-74-26, Interim Report, April, 1974.

6. McLean, A. F., Fisher, E. A., Bratton, R. J., "Brittle Materials Design, High Temperature Gas Turbine," AMMRC-74-59, Interim Report, September, 1974.

7. McLean, A. F., Fisher, E. A., Bratton, R. J., "Brittle Materials Design, High Temperature Gas Turbine," AMMRC-CTR-75-8, Interim Report, April, 1975.

8. McLean, A. F., Fisher, E. A., Bratton, R. J., Miller, D. G., "Brittle Materials Design, High Temperature Gas Turbine," AMMRC-CTR-75-28, Interim Report, September, 1975.

9. McLean, A. F., Baker, R. R., Bratton, R. J., Miller, D. G., "Brittle Materials Design, High Temperature Gas Turbine," AMMRC-CTR-76-12, Interim Report, April, 1976.

10. McLean, A. F., Baker, R. R., "Brittle Materials Design, High Temperature Gas Turbine," AMMRC-CTR-76-31, Interim Report, October, 1976.

11. McLean, A. F., Fisher, E. A., "Brittle Materials Design, High Temperature Gas Turbine," AMMRC-CTR-77-20, Interim Report, June, 1977.

12. McLean, A. F., Baker, R. R., "Brittle Materials Design, High Temperature Gas Turbine, Volume 1 Ceramic Component Fabrication and Demonstration," AMMRC-TR78-14, Interim Report, March, 1978.

13. McLean, A. F., Baker, R. R., "Brittle Materials Design, High Temperature Gas Turbine, Volume 2, Ceramic Turbine Rotor Technology," AMMRC-TR 78-14, Interim Report, March, 1978.

14. Thompson, D. O., Proceedings of the ARPA/AFML, Review of Progress in Quantitative NDE., AFML TR-78-55, May, 1978.

15. Thompson, D. O., Proceedings of the ARPA/AFML, Review of Progress in Quantitative NDE., AFML-TR-78-205, January, 1979.

16. Henry Ford Hospital, Detroit, Michigan.

17. G. N. Hounsfield, Br. J. Rad., **46**, pp. 1016-1022 (1973).

18. R. N. Bracewell, Aust. J. Phys., **9**, pp. 198-217 (1956).

19. D. J. DeRosier and A. Klug, Nature, **217**. pp. 130-134 (1968)

20. R. Gordon, R. Bender, and G. T. Herman, J. Theor. Biol., **29**, pp. 471-481, (1970).

21. G. N. Ramachandran and A. V. Lakshiminarayanan, Proc. Nat. Acad. of Sci., **68** pp. 2236-2240 (1971).

22. D. E. B. Lees, J. W. Keyes, and W. Simon, Proc. SPIE Conf. on Applic. of Opt. Inst. in Med. II, Palos Verdes, CA. (1973).

23. L. A. Shepp and B. F. Logan, IEEE Trans. Nuc. Sci., **NS-21** (3), pp. 21-43 (1974).

24. G. Tanaka and T. A. Iinuma, Phys. Med. Biol., **20**, pp. 789-798 (1975).

25. Z. H. Cho and I. Ahn, Comput. and Biol. Res., **8**, pp. 8-19 (1975).

26. G. T. Herman, A. Lent, and S. W. Rowland, J. Theor. Biol., **42**, pp. 1-23 (1973).

27. R. Gordon, IEEE Trans. Nuc. Sci., **NS-21** (3) pp. 78-91 (1974).

28. G. T. Herman and A. Lent, Comput. Biol. Med., **6**, pp. 273-311 (1976).

DISTRIBUTION

NO. OF COPIES	ORGANIZATION
12	Defense Documentation Center Cameron Station Alexandria, VA 22314
	Office of Naval Research Department of the Navy 800 N. Quincy Street Arlington, VA 22217
1	ATTN: Code 471
1	Code 102
1	Code 470
1	Commanding Officer Office of Naval Research Branch Office Building 114, Section D 666 Summer Street Boston, MA 02210
1	Commanding Officer Office of Naval Research Branch Office 536 South Clark Street Chicago, IL 60605
1	Office of Naval Research San Francisco Area Office One Hallidie Plaza Suite 601 San Francisco, CA 94102
	Naval Research Laboratory Washington, DC 20375
	ATTN: Codes 6000 6100 6300 6400 2627
1	Naval Air Development Center Code 302 Warminster, PA 18964 ATTN: Mr. F. S. Williams
1	Naval Air Propulsion Test Center Trenton, NJ 08628 ATTN: Library
1	Naval Construction Batallion Civil Engineering Laboratory Port Hueneme, CA 93043 ATTN: Materials Division
1	Naval Electronics Laboratory San Diego, CA 92152 ATTN: Electron Materials Sciences Division
1	Naval Missile Center Materials Consultant Code 3312-1 Point Mugu, CA 92041
1	Commanding Officer Naval Surface Weapons Center White Oak Laboratory Silver Spring, MD 20910 ATTN: Library
1	David W. Taylor Naval Ship Research and Development Center Materials Department Annapolis, MD 21402
1	Naval Undersea Center San Diego, CA 92132 ATTN: Library
1	Naval Underwater System Center Newport, RI 02840 ATTN: Library
1	Naval Weapons Center China Lake, CA 93555 ATTN: Library
1	Naval Postgraduate School Monterey, CA 93940 ATTN: Mechanical Engineering Department
1	Naval Air Systems Command Washington, DC 20360 ATTN: Codes 52031 52032
1	Naval Sea System Command Washington, DC 20362 ATTN: Code 035
1	Naval Facilities Engineering Command Alexandria, VA 22331 ATTN: Code 03

NO. OF COPIES	ORGANIZATION
1	Scientific Advisor Commandant of the Marine Corps Washington, DC 20380 ATTN: Code AX
1	Naval Ship Engineering Department of the Navy Washington, DC 20360 ATTN: Code 6101
1	Army Research Office P.O. Box 12211 Triangle Park, NC 27709 ATTN: Metallurgy & Ceramics Program
1	Army Materials and Mechanics Research Center Watertown, MA 02172 ATTN: Research Programs Office
	Air Force Office of Scientific Research Bldg. 410 Bolling Air Force Base Washington, DC 20332
1	ATTN: Chemical Science Directorate
1	Electronics & Solid State Sciences Directorate
1	Air Force Materials Laboratory Wright-Patterson AFB Dayton, OH 45433
1	Library Building 50, Rm 134 Lawrence Radiation Laboratory Berkeley, CA
1	NASA Headquarters Washington, DC 20546 ATTN: Code RRM
1	NASA Lewis Research Center 21000 Brookpark Road Cleveland, OH 44135 ATTN: Library
	National Bureau of Standards Washington, DC 20234
1	ATTN: Metallurgy Division
1	Inorganic Materials Div.

NO. OF COPIES	ORGANIZATION
1	Director Applied Physics Laboratory University of Washington 1013 Northeast Forthieth Street Seattle, WA 98105
1	Defense Metals and Ceramics Information Center Battelle Memorial Institute 505 King Avenue Columbus, OH 43201
1	Metals and Ceramics Division Oak Ridge National Laboratory P.O. Box X Oak Ridge, TN 37380
1	Los Alamos Scientific Laboratory P.O. Box 1663 Los Alamos, NM 87544 ATTN: Report Librarian
1	Argonne National Laboratory Metallurgy Division P.O. Box 229 Lemont, IL 60439
1	Brookhaven National Laboratory Technical Information Division Upton, Long Island New York 11973 ATTN: Research Library
1	Office of Naval Research Branch Office 1030 East Green Street Pasadena, CA 91106
1	Dr. F. F. Lange Rockwell International P.O. Box 1085 1049 Camino Dos Rios Thousand Oaks, CA 91360
1	Dr. J. Lankford Southwest Research Institute 8500 Culebra Road San Antonio, TX 78284
1	Library Norton Company Industrial Ceramics Division Worcester, MA 01606

NO. OF COPIES	ORGANIZATION
1	State University of New York College of Ceramics at Alfred University Alfred, NY 14802 ATTN: Library
1	Dr. L. Hench University of Florida Ceramics Division Gainesville, FL 32601
1	Dr. N. MacMillan Materials Research Laboratory Pennsylvania State University College Park, PA 16802
1	Mr. F. Markarian Naval Weapons Center China Lake, CA 93555
1	Dr. Perry A. Miles Raytheon Company Research Division 28 Seyon Street Waltham, MA 02154
1	Mr. R. Rice Naval Research Laboratory Washington, DC 20375 ATTN: Code 6360
1	Dr. J. Ritter University of Massachusetts Department of Mechanical Engineering Amherst, MA 01002
1	Professor R. Roy Pennsylvania State University Materials Research Laboratory University Park, PA 16802
1	Dr. R. Ruh AFML Wright-Patterson AFB Dayton, OH 45433
1	Mr. J. Schuldies AiResearch Phoenix, AZ
1	Professor G. Sines University of California, Los Angeles Los Angeles, CA 90024

NO. OF COPIES	ORGANIZATION
1	Dr. N. Tallan AFML Wright-Patterson AFB Dayton, OH 45433
1	Dr. T. Vasilos AVCO Corporation Research and Advanced Development Division 201 Lowell Street Wilmington, MA 01887
1	Mr. J. D. Walton Engineering Experiment Station Georgia Institute of Technology Atlanta, GA 30332
1	Dr. S. M. Widerhorn Inorganic Materials Division National Bureau of Standards Washington, DC 20234
1	Dr. W. F. Adler Effects Technology Inc. 5383 Hollister Avenue P.O. Box 30400 Santa Barbara, CA 92105
1	Dr. G. Bansal Battelle 505 King Avenue Columbus, OH 43201
1	Dr. R. Bratton Westinghouse Research Lab. Pittsburgh, PA 15235
1	Dr. A. G. Evans Rockwell International P.O. Box 1085 1049 Camino Dos Rios Thousand Oaks, CA 91360
1	Mr. E. Fisher Ford Motor Co. Dearborn, MI 48121
1	Dr. P. Gielisse University of Rhode Island Kingston, RI 02881
1	Dr. M. E. Gulden International Harvester Company Solar Division 2200 Pacific Highway San Diego, CA 92138

NO. OF COPIES	ORGANIZATION
1	Dr. D. P. H. Hasselman Montana Energy and MHD Research and Development Institute P.O. Box 3809 Butte, Montana 59701
1	Mr. G. Hayes Naval Weapons Center China Lake, CA 93555
1	Professor A. H. Heuer Case Western Reserve University University Circle Cleveland, OH 44106
1	Dr. R. Hoagland Battelle 505 King Avenue Columbus, OH 43201
1	Dr. R. Jaffee Electric Power Research Institute Palo Alto, CA 94301
1	Dr. P. Jorgensen Stanford Research Institute Poulter Laboratory Menlo Park, CA 94025
1	Dr. R. N. Katz Army Materials and Mechanics Research Center Watertown, MA 02171
1	Dr. H. Kirchner Ceramic Finishing Company P.O. Box 498 State College, PA 16801
1	Dr. B. Koepke Honeywell, Inc. Corporate Research Center 500 Washington Avenue, South Hopkins, MN 55343
1	Mr. Frank Koubek Naval Surface Weapons Center White Oak Laboratory Silver Spring, MD 20910
1	E. Krafft Carborundum Co. Niagara Falls, NY 14301

NO. OF COPIES	ORGANIZATION
1	Dr. S. A. Bortz IITRI 10 W. 35th Street Chicago, IL 60616
1	Mr. G. Schmitt Air Force Materials Laboratory Wright-Patterson AFB Dayton, OH 45433
1	Dr. D. A. Shockey Stanford Research Institute Poulter Laboratory Menlo Park, CA 94025
1	Dr. W. G. D. Frederick Air Force Materials Laboratory Wright-Patterson AFB Dayton, OH 45433
1	Dr. P. Land Air Force Materials Laboratory Wright-Patterson AFB Dayton, OH 45433
1	Mr. K. Letson Redstone Arsenal Huntsville, AL 35809
1	Dr. S. Freiman Naval Research Laboratory Washington, DC 20375 ATTN: Code 6363
1	Director Materials Sciences Defense Advanced Research Projects Agency 1400 Wilson Boulevard Arlington, VA 22209
1	Dr. James Pappis Raytheon Company Research Division 28 Seyon Street Waltham, MA 02154
1	Major W. Simmons Air Force Office of Scientific Research Building 410 Bolling Air Force Base Washington, DC 20332

NO. OF COPIES	ORGANIZATION
1	Dr. P. Becher Naval Research Laboratory Washington, DC 20375 ATTN: Code 6362
1	Mr. L. B. Weckesser Applied Physics Laboratory Johns Hopkins Road Laurel, MD 20810
1	Mr. D. Richardson AiResearch Manufacturing Company 4023 36th Street P.O. Box 5217 Phoenix, AZ 85010
1	Dr. H. E. Bennett Naval Weapons Center China Lake, CA 93555 ATTN: Code 3818
1	Mr. G. Denman Air Force Materials Laboratory Wright-Patterson AFB Dayton, OH 45433 ATTN: Code LPJ
1	Dr. D. Godfrey Admiralty Materials Laboratory Polle, Dorset BH16 6JU UNITED KINGDOM
1	Dr. N. Corney Ministry of Defense The Adelphi John Adam Street London WC2N 6BB UNITED KINGDOM
1	Dr. L. M. Gillin Aeronautical Research Laboratory P.O. Box 4331 Fisherman's Bend Melbourne, VIC 3001 AUSTRALIA
1	Dr. G. Ewell MS6-D163 Hughes Aircraft Co. Centinela and Teale Streets Culver City, CA 90230

NO. OF COPIES	ORGANIZATION
1	Dr. R. E. Tressler Ceramic Science Section 226 Steidle Bldg. The Pennsylvania State Univ. University Park, PA 16802
1	Dr. R. E. Newnham Materials Research Laboratory The Pennsylvania State University University Park, PA 11802
1	Dr. F. F. Lange Rockwell International Science Center 1049 Camino Dos Rios Thousand Oaks, CA 91360
1	Dr. K. D. McHenry Honeywell, Inc. Corporate Technology Center 10701 Lyndale Avenue South Bloomington, MN 55420
1	Dr. N. H. Macmillan Materials Research Laboratory The Pennsylvania State University University Park, PA 16802
1	Dr. R. A. Queeney Professor of Engineering Mechanics Hammond Bldg. The Pennsylvania State University University Park, PA 16802
1	Dr. George W. Taylor Princeton Resources, Inc. P.O. Box 211 Princeton, New Jersey 08540
1	Dr. Herb Moss RCA Laboratories Princeton, New Jersey 08540